UNIVERSIDADE FEDERAL DO CEARÁ
CENTRO DE TECNOLOGIA
CURSO DE ENGENHARIA DE PETRÓLEO

TÁCITO SAMPAIO GASPAR DE OLIVEIRA FILHO

STUDY OF THE FORMATION AND INHIBITION OF MINERAL SCALES USING A HANDCRAFTED ACRYLIC POROUS MODEL

FORTALEZA

2017

TÁCITO SAMPAIO GASPAR DE OLIVEIRA FILHO

STUDY OF THE FORMATION AND INHIBITION OF MINERAL SCALES USING A HANDCRAFTED ACRYLIC POROUS MODEL

Monography presented to the Petroleum Engineering course of the Universidade Federal do Ceará in 2017, as a partial request for obtaining the title of Bachelor of Petroleum Engineering.

Supervisor: Prof. Dr. Francisco Murilo Tavares de Luna.

FORTALEZA

2017

Dados Internacionais de Catalogação na Publicação
Universidade Federal do Ceará
Biblioteca Universitária
Gerada automaticamente pelo módulo Catalog, mediante os dados fornecidos pelo(a) autor(a)

O52s Oliveira Filho, Tácito Sampaio Gaspar de.
Study of the formation and inhibition of mineral scales using a handcrafted acrylic porous model / Tácito Sampaio Gaspar de Oliveira Filho. – 2017.
46 f. : il. color.

Trabalho de Conclusão de Curso (graduação) – Universidade Federal do Ceará, Centro de Tecnologia, Curso de Engenharia de Petróleo, Fortaleza, 2017.
Orientação: Prof. Dr. Francisco Murilo Tavares de Luna.

1. Mineral scales. 2. Inhibitors. 3. Porous chip. I. Título.

CDD 665.5092

TÁCITO SAMPAIO GASPAR DE OLIVEIRA FILHO

STUDY OF THE FORMATION AND INHIBITION OF MINERAL SCALES USING A HANDCRAFTED ACRYLIC POROUS MODEL

Monography presented to the Petroleum Engineering course of the Universidade Federal do Ceará in 2017, as a partial request for obtaining the title of Bachelor of Petroleum Engineering.

Supervisor: Prof. Dr. Francisco Murilo Tavares de Luna

Approved on: ___/___/_____.

EXAMINING BOARD

_____
Prof. Dr. Francisco Murilo Tavares de Luna (Orientador)
Universidade Federal do Ceará (UFC)

_____
M.Sc. Arthur Reys Carvalho de Oliveira
Universidade Federal do Ceará (UFC)

_____
Eng. Vanessa Fernandes de Oliveira
Universidade Federal do Ceará (UFC)

To God.

To my parents, Tácito and Vládia.

ACKNOWLEDGEMENTS

To my family for all the support they gave me during this journey. Special thanks to my mother Vládia Rios, to my father Tácito Sampaio, and to my grandmother Goretti Rios for all the help they offered to me.

Thanks to my girlfriend Isabelle for being with me during all the years of my graduation in Brazil and Australia.

I would like to thank all of my friends that were with me during this part of my life. Otto Bessa, Wilson Carvalho, Rodrigo Machado, Leonardo Sales, Jéssica Oliveira, Milena Buendia, Leonardo de Abreu, Renan Ozório and Isabela Vieira, without you this graduation would have been undoubtfully more difficult.

Thanks to CNPq for the scholarships in the programs Jovens Talentos para a Ciência, Ciência Sem Fronteiras, e PIBIC. These programs were of incredible importance for my academic development and for my life.

I would like to thank my professors and supervisors during my graduation at UFC and at my study abroad period at UNSW, Australia.

Thanks to my supervisor Prof. Dr. Franscisco Murilo Tavares de Luna for all the support in this final step of my formation.

Thanks to the members of the examining board.

“If I have seen further than others, it is by standing upon the shoulders of giants”
Isaac Newton

ABSTRACT

Mineral scales in the oil field is one of the major industry problems. It usually forms when two incompatible waters, normally formation water and injection water, enter in contact inside the reservoir rock or in the production tubing and sulfate (SO_4^{2-}) and carbonate (CO_3^{2-}) salts precipitates. The precipitation is usually resolved using an inhibitor that is pumped with the injection water in a process known as a *squeeze* treatment. In this work, an acrylic medium was designed and manufactured to study the precipitation and inhibition of these salts. Two saline waters – one containing sulfate and carbonate ions, and the other containing magnesium, calcium, strontium, barium and potassium ions – were produced, mixed and pumped inside an acrylic medium to study how these scales form and how to inhibit them using various concentrations (1, 2, 4, 8 and 16ppm) of ATMP (aminotris(methylenephosphonic acid)). The runs were analyzed using a microscope and a Graph showing the correlation between the concentration of ATMP and the time it took to reach 30 psi inside the acrylic medium. The results show a clear correlation between the concentration of the inhibitor and the time it takes for the scales to form.

Keywords: Mineral scales. Inhibitors. Porous chip.

RESUMO

Incrustações minerais nos campos de petróleo são uns dos principais problemas da indústria. Usualmente essas incrustações formam-se quando duas águas incompatíveis, normalmente água de formação e água de injeção, entram em contato dentro da rocha reservatório ou na linha de produção e sais de sulfato (SO_4^{2-}) e carbonato (CO_3^{2-}) precipitam. A precipitação é normalmente resolvida utilizando um inibidor que é bombeado com a água de injeção em um processo conhecido como tratamento *squeeze*. Neste trabalho, um chip de acrílico foi projetado e produzido para estudar a precipitação e inibição destes sais. Duas soluções salinas – uma contendo íons sulfato e carbonato, e outra contendo íons magnésio, cálcio, estrôncio, bário e potássio – foram produzidas, misturadas e bombeadas para o chip de acrílico para estudar como estas incrustações formam-se e como inibi-las utilizando várias concentrações (1, 2, 4, 8 e 16ppm) de ATMP (aminotris(ácido trimetilfosfônico)). Os testes foram analizados utilizando um microscópio e gráficos mostrando a relação entre a concentração de ATMP e o tempo necessário para atingir 30psi dentro do chip de acrílico. Os resultados mostram uma clara relação entre a concentração do inibidor e o tempo que leva até as incrustações se formarem.

Palavras-chave: Incrustações minerais. Inibidores. Chip poroso.

LIST OF FIGURES

LIST OF GRAPHS

LIST OF TABLES

ABBREVIATIONS

ATMP	Aminotris(methylene-phosphonic acid)
DN	Nominal diameter
DTPMP	Diethylenetriaminepenta(methylene-phosphonic acid)
ID	Inner diameter
OD	Outer diameter
Penta	Diethylenetriaminepenta(methylene-phosphonic acid)
TBT	Tube-blocking test
Tris	Aminotris(methylene-phosphonic acid)

LIST OF SYMBOLS

Ba	Barium
°C	Celsius degrees
C	Carbon
Ca	Calcium
Cl	Chloride
cm	Centimeter
g	Grams
H	Hydrogen
in	Inches
K	Potassium
kg	Kilograms
L	Liters
m	Meters
Mg	Magnesium
min	Minutes
ml	Milliliters
mm	Millimeters
N	Nitrogen
Na	Sodium
O	Oxygen
ppm	Parts per million
psi	Pounds per square inch
psia	Pounds per square inch absolute
psig	Pounds per square inch gauge
S	Sulphur
Sr	Strontium
µm	Micrometers
%	Percentage
®	Registered trademark

SUMMARY

1 INTRODUCTION

The petroleum industry is one of the biggest and most lucrative industries of the world. But that comes with very serious problems that can completely destroy a multi-billion-dollar investment. One of these problems is the precipitation of salts and, consequently, the formation of mineral scales (TOMSON, FU, *et al.*, 2002).

These scales can form on almost all of the steps of the petroleum extraction, the most serious and most expensive places are on the production and transport tubing. Those tubes cost several million dollars to replace, and to perform the replacement the production needs to stop completely, meaning that a potential of millions of dollars per day is being lost (MERDHAH, 2007).

The precipitation of these salts occurs when two incompatible waters mix together, causing the nucleation of salts very insoluble in water. Normally, those waters are called injection water and formation water.

Formation water is the water inside the reservoir rock, usually in the pores of the rock with the oil or beneath the reservoir inside an adjacent aquifer. Those waters normally contain very high salt contents, with Sodium, Magnesium, Calcium, Barium and Strontium being among the ions with high concentrations. The Figure 1 shows the location of the formation water in the petroleum reservoir (MERDHAH, 2007) (ODDO, SMITH e TOMSON, 1991).

Figure 1 - Conventional petroleum reservoir

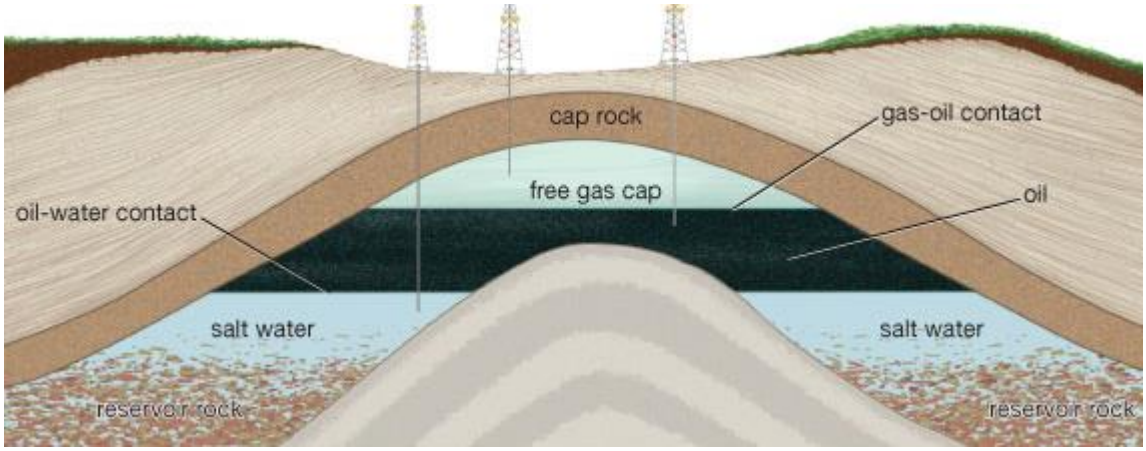

Source: Encyclopædia Britannica – Gas Reservoir (adapted), accessed on 17 December, 2017.

Injection water, as the name suggests, is the water that is pumped inside the production string or the reservoir rock. It serves the purpose to maintain the hydrostatic pressure in the production string or to provide additional pressure for the oil to reach the surface, as in a secondary recovery method. It is normally just sea water but synthetic brines are also used by the industry (MERDHAH, 2007) (CROWE, MCCONNELL, *et al.*, 1994).

Usually, seawater contains SO_4^{2-} and CO_3^{2-} ions. Those ions when combined with the ones present in the formation water, precipitates sulfate and carbonate salts. Those salts are very insoluble in water, making it very easy for deposition and formation of mineral scales (MILLERO, 2006) (MERDHAH, 2007).

To prevent the formation of mineral scales, various inhibitors are used by the industry, two of the most common are aminotris(methylene-phosphonic acid), also known as Tris or ATMP, and diethylenetriaminepenta(methylene-phosphonic acid), also known as Penta or DTPMP. Those inhibitors are pumped with the injection water in what is called a squeeze treatment (VELOSO, 2017) (OLIVEIRA, 2017) (CROWE, MCCONNELL, *et al.*, 1994).

To study the formation and inhibition of these mineral scales, several methods were developed by the petroleum industry, we have tube blocking tests, pore network modeling, core flooding tests, and porous chips tests (BARTOLOMEU, 2017).

The objective of this work is to develop and manufacture an acrylic porous medium to study both quantitatively and qualitatively the formation and inhibition of mineral scales using two synthetic brines to represent the formation and injection water, and using ATMP as the inhibitor.

2 LITERATURE REVIEW

2.1 Mineral scales formation

One of the most important aspects of oil wells is the persistent problem of scale formation. This problem exists during production, treatment, transportation, and disposal of the water that is produced with the hydrocarbons in a petroleum reservoir (TOMSON, FU, WATSON, 2012).

Scales are formed by many minerals, but the most common are Calcite ($CaCO_3$), Barite ($BaSO_4$), gypsum and others minerals related to calcium sulfates ($CaSO_4.xH_2O$). There are also scales that does not come from minerals, such as those that come from hydrocarbon-based deposits. They can assume the form of gas hydrates, waxes, asphalthenes, naphthenates, and sulfur (TOMSON, FU, WATSON, 2012). Figure 2 shows the magnitude of what some of those scales structures can achieve.

Figure 2 - Barium Sulfate Scale

Source: FQE Chemicals – Barium Sulfate Scale, accessed on 15 December, 2017.

Many oil wells have some kind of flow obstruction. The main cause is scale deposition. Specially in wells where seawater is injected to maintain the pressure in the reservoir and to improve secondary recovery. This operation is very mature and has been studied extensively by the industry (MERDHAH, 2007).

The main reason that mineral scales are undesirable is because it reduces the flow diameter of the production or transport tubing. This reduction causes a rise in pressure loss in the oil extraction line, reducing the flow rate of oil (OLIVEIRA, 2017).

Scale formation has two basic origins: organic or inorganic. The organic usually comes from the hydrocarbons, creating deposits of paraffins, asphalthenes, hydrates, and naphthenes. And the inorganic scales come from the precipitation of salts of carbonates, sulfates, sulfites, oxides, hydroxides and silicates (OLIVEIRA, 2017).

In the oil industry, the two most common inorganic scales come from the precipitation of carbonates and sulfates (COSMO, 2013).

2.1.1 Carbonate precipitation and scale formation

Calcium carbonate is an inorganic salt that forms when we have an aqueous ambient saturated with carbonate (CO_3^{2-}) and calcium (Ca^{2+}) ions. Initially, small solid particles are formed, that constructs a group following an order, giving origin to a mineral. The ordering of the particles in the mineral changes the mineral nomenclature, it can be called calcite, aragonite, vaterite, etc. The calcite is the mineral most commonly found, because it is the most sTable (COSMO, 2013). The Equation 1 shows the formation of the calcium carbonate. The Figure 3 shows the characteristics of the calcium carbonate ($CaCO_3$) scales.

$$Ca^{2+}_{(aq)} + {CO_3^{2-}}_{(aq)} \leftrightharpoons CaCO_{3(s)} \quad (1)$$

Figure 3 - Calcium carbonate scale in pipe

Source: Aquatekpro – Scale Control, accessed on 15 December, 2017.

The process of the first grouping of solid particles is called nucleation. The grouping of new ions and/or new particles consists in a process called solid growth. The most important factors for the formation of calcium carbonate are the saturation of carbonate and calcium ions, and CO_2 loss from the aqueous solution. The Equation bellow shows this mechanism of the sequence of formation of this solid (COSMO, 2013).

$$Ca^{2+} + 2HCO_3^- \leftrightharpoons CaCO_3 + H_2O + CO_2 \quad (2)$$

However, the formation of the calcium carbonate salt it's not so simple as Equation 2 indicates, other ions in the solution, as H^+, OH^-, $CaOH^+$ and $CaHCO_3^+$, affect the formation of this compound. Other studies show that hydroxonium (H_3O^+) and carbonic acid (H_2CO_3) also changes the kinetic of the reaction (COSMO, 2013). Those effects are show in Equations 3 to 5.

$$CO_2 + 2H_2O \leftrightharpoons HCO_3^- + H_3O^+ \quad (3)$$

$$CO_2 + H_2O \leftrightharpoons H_2CO_3 \quad (4)$$

$$H_2O \leftrightharpoons H^+ + OH^- \quad (5)$$

The variables that affect the precipitation of carbonates are temperature, pressure, carbon dioxide presence and partial pressure, pH, ionic forces, Ca^{2+} concentration, alkalinity and the presence of other ions, such as Mg^{2+} and SO_4^{2-}. We can see that the reaction is in equilibrium and the addition or subtraction of chemical compounds will cause a shift in the reaction equilibrium. This is improbable in a petroleum reservoir, so only the pressure and temperature variation will affect the reaction equilibrium constant, giving the force to start the deposition of calcium carbonate (OLIVEIRA, 2017).

The effect of CO_2 on the precipitation of $CaCO_3$ is shown in Figure 4. We can see that increasing the concentration of CO_2 will decrease the amount of solid calcium carbonate. The rise in temperature makes the precipitation increase, because the increase in temperature decreases the solubility of $CaCO_3$. The Figure 5 shows the effect of the CO_2 partial pressure, we can see that we have an decrease in deposition when we increase the partial pressure of carbon dioxide (COSMO, 2013) (OLIVEIRA, 2017).

Figure 4 - Calcite solubility for 50 and 100°C in function of CO2 total in solution

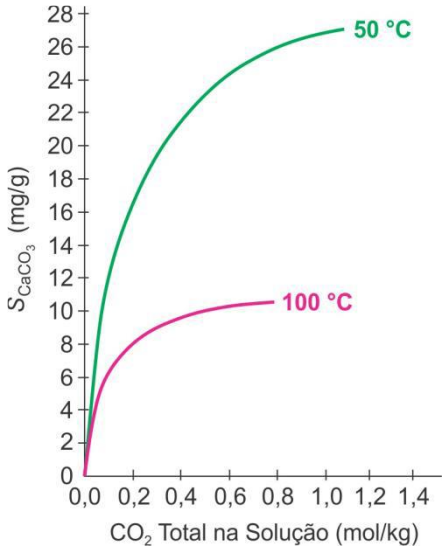

Source: COSMO, 2013 ; DUAN and LI, 2008.

Figure 5 - Calcite solubility for 100°C in function of CO2 partial pressure

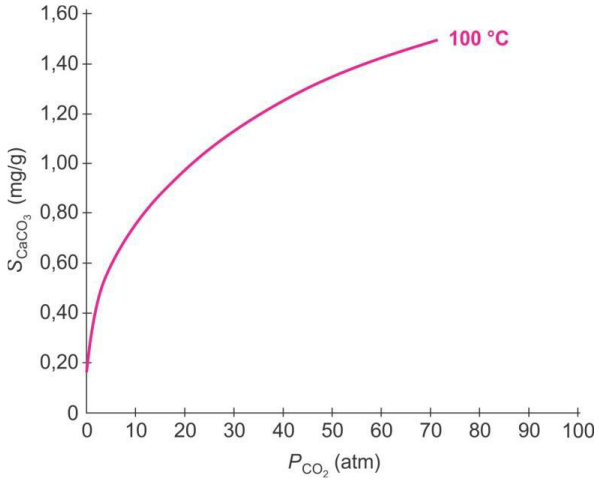

Source: COSMO, 2013 ; SEGNIT, 1962.

The increase in temperature makes the solubility of the calcium carbonate decrease. This is because the rise in temperature dissolves more ions, making, for some salts, the solubility decrease (MERDHAH, 2007).

Considering that the temperature at sea level is 25°C and the temperature at the reservoir varies between 50 and 200°C, we can see that we have a great temperature variation, so this is one of the most important factors in calcium carbonate precipitation (OLIVEIRA, 2017). We can see the temperature effect in Figure 6.

Figure 6 - Relation between the solubility of $CaCO_3$ and the temperature

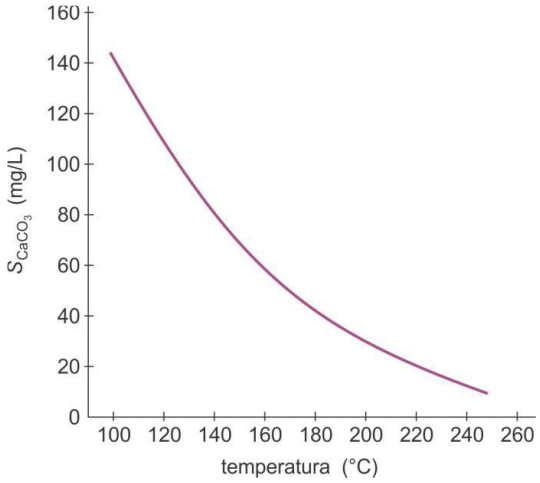

Source: COSMO, 2013 and POOL, RANEY, SHANNON, 1987.

The pressure has the opposite effect of the temperature, making the solubility of calcium carbonate increase with the increment in pressure. This is because the content of the precipitation of $CaCO_3$ with the decrease in pressure is because of CO_2 flash and the direct reduction of the mineral solubility (COSMO, 2013). We can see the effect of pressure in Figure 7.

Figure 7 - CaCO3 solubility at 100°C in function of the system pressure

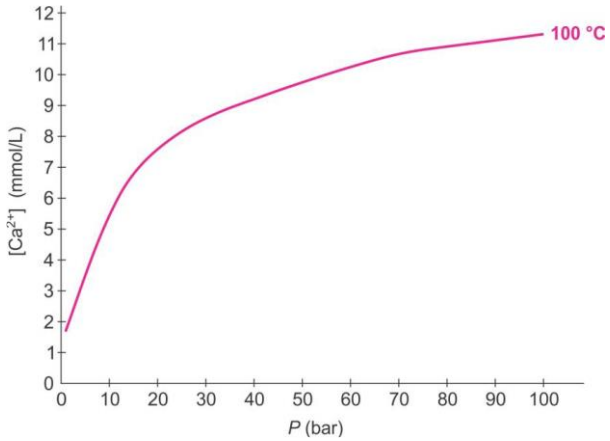

Source: COSMO, 2013 and COTO et al., 2012.

2.1.2 Sulfate precipitation and scale formation

The most common sulfate scales are the ones formed with calcium, barium and strontium. Forming Calcium Sulfate ($CaSO_4$), Barium Sulfate ($BaSO_4$) and Strontium Sulfate ($SrSO_4$).

Calcium sulfate occurs in three different phases and can exist in several crystalline forms, including gypsum ($CaSO_4.2H_2O$) and anhydrite ($CaSO_4$) (MERDHAH, 2007).

At a lower temperature the most common scale is the gypsum, but at a higher temperature the stable predicted phase is anhydrite. The other phase, hemihydrate ($CaSO_4.1/2H_2O$) has been known to form at 100 to 121°C (MERDHAH, 2007).

The reaction of the precipitation of calcium sulfate is shown in Equation 6.

$$Ca^{2+} + SO_4^{2-} \leftrightharpoons CaSO_4 \tag{6}$$

According to Oddo et al., calcium sulfate scale formation is somewhat dependent on temperature, but is typically precipitated because of a decrease in pressure or an increase in the relative concentrations of calcium or sulfate. As for the pH, the solubility is independent and $CaSO_4$ can precipitate in an acid environment (ODDO, SMITH e TOMSON, 1991) (MERDHAH, 2007).

The scales of barium sulfate ($BaSO_4$) is a disaster in waterflooding projects, because of the incompatible waters, the formation and injection water. This results in heavy precipitation and consequent permeability reduction. It is the most insoluble scale that can be precipitated from oilfield water. The scale has a very high hardness and is very difficult to remove (MERDHAH, 2007).

The reaction of the precipitation of barium sulfate is shown in Equation 7.

$$Ba^{2+} + SO_4^{2-} \leftrightharpoons BaSO_4 \tag{7}$$

The solubility of barium sulfate goes up with increasing temperature, pressure and salt content of the brine. Thus, prediction of barium sulfate scale is much easier than the other since a pressure, temperature or salt content drop will increase precipitation (MERDHAH, 2007).

Until recently, the appearance of strontium in oilfield scales has been primarily in the presence of barium sulfate scale. But is being observed that almost pure $SrSO_4$ is being deposited in production wells around the world. The most common mechanism for these scales to form is the result of subsurface commingling of waters, resulting in a supersaturation of strontium sulfate.

Strontium sulfate behaves like barium sulfate except the former is more soluble under the same conditions. Almost all oilfields that contain $BaSO_4$ also contain $SrSO_4$ (MERDHAH, 2007). The reaction of strontium sulfate precipitation is shown in Equation 8.

$$Sr^{2+} + SO_4^{2-} \leftrightharpoons SrSO_4 \quad (8)$$

2.2 Mineral scale inhibition

The majority of mineral scales inhibitors have an active phase of the phosphonic acid class. Inside this class, we opted to use the inhibitor aminotris-methylenephosphonic acid (ATMP) (VELOSO, 2017). We can see the molecular structure of the inhibitor in Figure 8.

Figure 8 - ATMP acid molecular structure

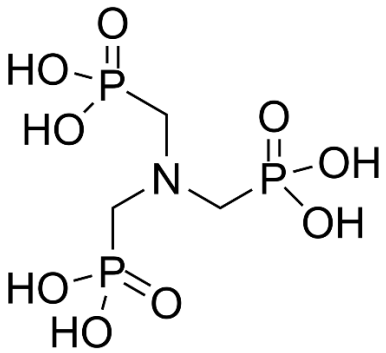

Source: Wikipedia – ATMP, accessed on 16 December, 2017.

The mineral scales inhibitors have the function to prevent the deposition of inorganic salts on the tubing walls of the petroleum production system. Acting on the thermodynamic stability, inhibiting the nucleation or interfering in the process of crystal growth, blocking the expansion of the crystal (OLIVEIRA, 2017) (MERDHAH, 2007).

To be a good scale inhibitor, is necessary for a chemical compound that it have a good water affinity, good resistance for field usage, and high efficiency actuating in the deposition of these scales. That means that the inhibitor needs to have groups that can form bonds with cations, such as carboxylic acid, sulfonic acid or phosphonic acid groups. These groupings can facilitate the bonding with metallic cations, lowering the concentration and stopping the deposition of these mineral scales (OLIVEIRA, 2017).

Methylene phosphonic acid have been widely used in precipitation squeeze treatments. Some papers described the use of ATMP in carbonate formations in Saudi Arabia

and reported the scale protection was active for the excess of 1000 production days (CROWE, MCCONNELL, *et al.*, 1994).

Laboratory micromodel studies show that the inhibitor return rate is reduced by trapping the precipitated inhibitor in certain pores of the rock. The slower dissolution appears to result from mass transfer limitations caused by partial plugging of some pore throats by the precipitate. Another factor which slows inhibitor dissolution is influence of common ions on the solubility of the precipitated inhibitor (CROWE, MCCONNELL, *et al.*, 1994).

An additional factor which may extend the effective life of inhibitor squeeze treatments is the rise of the water level in the producing zone. During a squeeze treatment, the inhibitor is injected into the entire perforated interval. If water production predominantly occurs from the lower section of this interval, the scale inhibitor will initially be preferentially extracted from this section (CROWE, MCCONNELL, *et al.*, 1994).

2.3 Porous media chip

The main focus of this work is to study the mineral scale inhibition inside a porous media. One of the most famous artificial porous media is the Dolomite® Porous Media Chip. Very few studies have been made using acrylic chips to study the action of ATMP on the mineral scale inhibition.

The porous media chip is a glass microfluidic device designed for statistically representative modelling of a complex porous sandstone rock structure. Applications include academic research (earth science and engineering), petrochemical industry, and environmental testing and groundwater analysis (DOLOMITE, 2017).

The Figure 9 shows the pore structure of the porous media chip.

With the objective of analyzing the displacement of oil using injections of polymeric solutions in pore scale, Lima and Carvalho used a device of microfluidics that artificially reproduces a porous medium. Their work was developed using the geometric parameters of the micromodel showed above, in Figure 9 (BARTOLOMEU, 2017).

Figure 9 - A top-down diagram explaining the chip structure

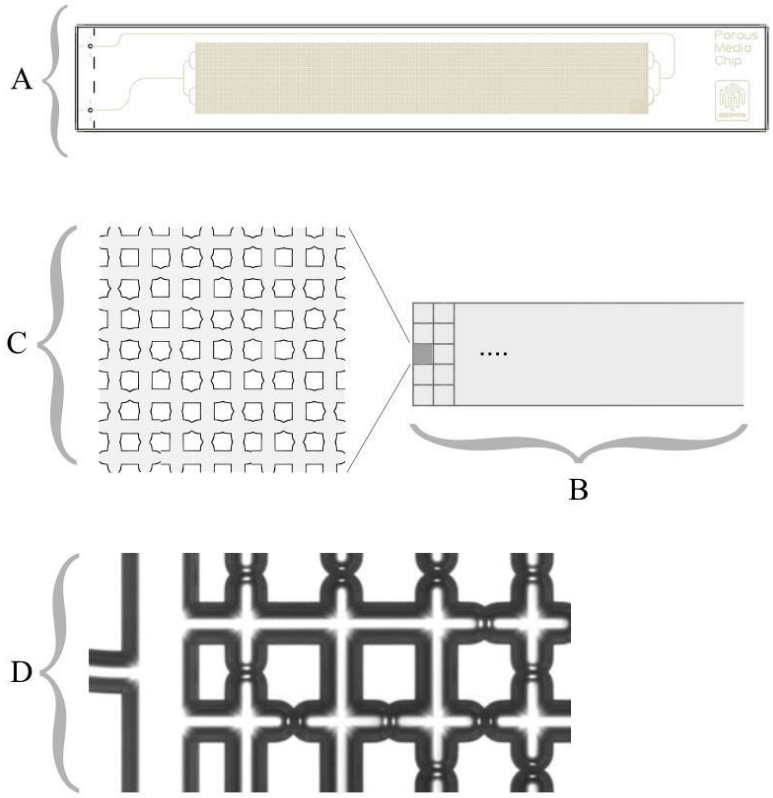

Source: DOLOMITE, 2017.

Newer techniques of image analysis have been developed with the objective of representing the geometry and topology of a porous medium in different types of rock. The development of geometrical descriptions is becoming more realistic as the time passes. The Figure 10 shows a model of a sandstone pore structure (BARTOLOMEU, 2017).

Figure 10 - (a) Representation of a porous rock (b) Capillary network

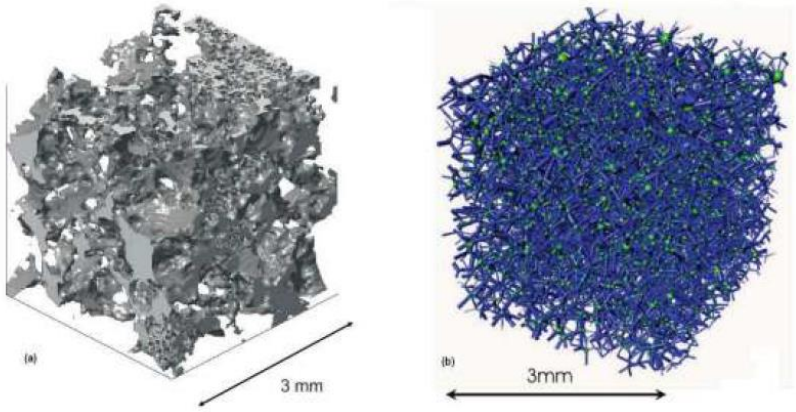

Source: BARTOLOMEU, 2017 and ØREN, BAKKE, 2003.

Fatt's work showed that studying different processes of displacement in porous medium have been possible because of the ample usage of models of capillary network. Blunt and King developed a model of an hexagonal network and, after that, a model of a network in pore scale was developed where the pores were modeled as spheres and the throats as cylindrical tubes (FATT, 1956) (BLUNT e KING, 1992) (BARTOLOMEU, 2017).

2.4 Literature results

Oliveira tested dynamic efficiency using the Tube Blocking Test (TBT) to see the efficiency of chemical inhibitors to prevent the formation and deposition of mineral scales, such as calcium carbonate. He tested the solutions showed in Tables 1 and 2 for a temperature of 100°C, a pressure of 80 bar and an injection rate of 10 mL/min. Using a capillary tube with 1m length and 0.25mm of diameter. He obtained the results showed in Figure 11 for the ATMP inhibitor (OLIVEIRA, 2017).

Table 1 - Brine 1

Ions	g/L
Na^{+}	49.594
Mg^{2+}	4.432
Ca^{2+}	7.484
K^{+}	2.078
Sr^{2+}	0.882
Ba^{2+}	1.014

Source: OLIVEIRA, 2017 and KELLAND, 2011.

Table 2 - Brine 2

Ions	g/L
Na^{+}	49.594
HCO_3^{-}	2.752

Source: OLIVEIRA, 2017 and KELLAND, 2011.

Figure 11 - Performance of ATMP in TBT method

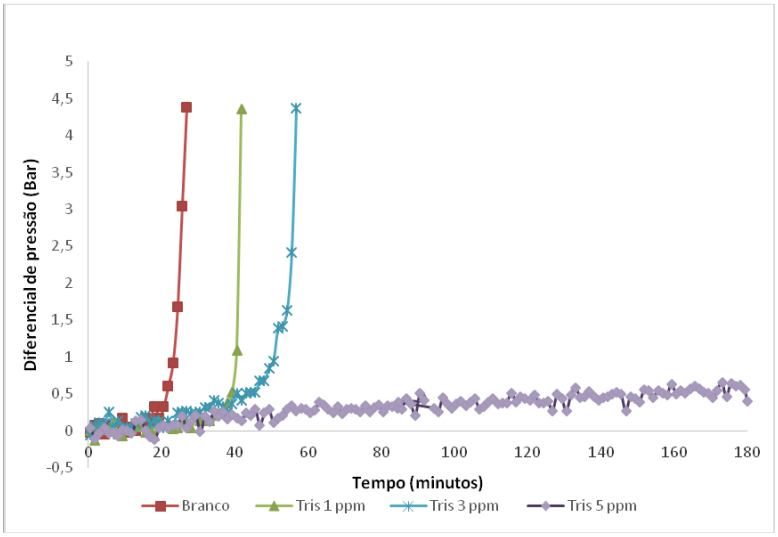

Source: OLIVEIRA, 2017.

Merdhah used four types of formation water, two with high salinity and two with high barium concentration, and one type of injection water, containing the average salt content of Barton and Angsi seawaters, this is shown in Table 3. He injected both waters using different temperatures and pressures and obtained results for the permeability loss inside the rock. The obtained results are shown in Figures 12 and 13 (MERDHAH, 2007).

Table 3 - Compounds of synthetic formation and injection waters

Compound	**Normal salinity formation water (ppm)**	**High salinity formation water (ppm)**	**Normal barium formation water (ppm)**	**High barium formation water (ppm)**	**Average between Barton and Angsi seawaters (ppm)**
Sodium Chloride	132,000	132,000	106,500	106,500	26,100
Potassium Sulfate	-	-	-	-	5,180
Magnesium Chloride	35,625	35,625	853	853	9,846
Calcium Chloride	25,677	110,045	-	-	-
Sodium Bicarbonate	482	482	-	-	-
Strontium Chloride	1,521	3,347	-	-	-
Barium Chloride	-	-	445	3,914	-

Source: MERDHAH, 2007.

Figure 12 - Variation of permeability ratio as a function of time showing the effect of concentration at 100psig and 50°C

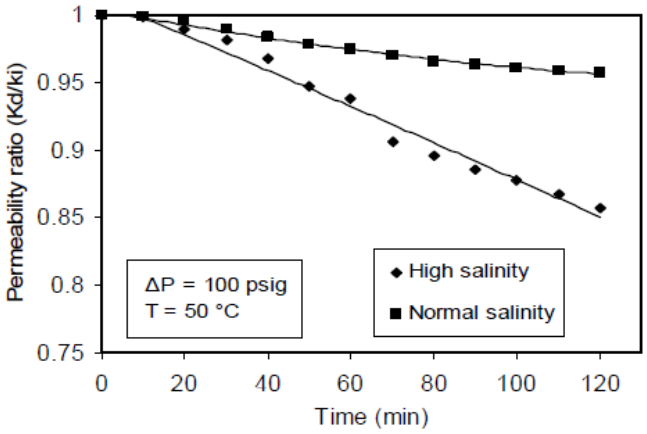

Source: MERDHAH, 2007

Figure 13 - Variation of permeability ratio as a function of time showing the effect of concentration at 200psig and 80°C

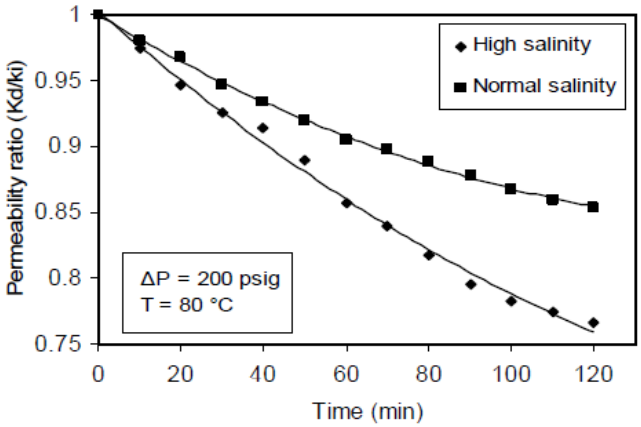

Source: MERDHAH, 2007

3 METHODOLOGY

3.1 Handcrafted acrylic porous medium

To study the formation and inhibition of mineral scales, an acrylic porous medium was designed and built. This device was based in the product sold by Dolomite®, the Porous Media Chip.

The first step in building the device was designing it in AutoCAD. Several designs were sketched, but the final iteration, used for the experiment is shown in Figure 14.

Figure 14 - AutoCAD vector drawing

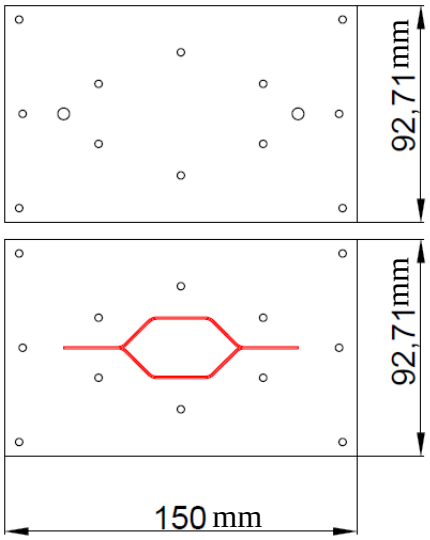

Source: Author (2017).

The model consists of two pieces, both with the dimensions of 150mm x 92.71mm, both with 12 holes with diameter of 1/8in, and the top piece have 2 extra holes with diameter of 3/16in, for the tubbing connections.

The bottom part has the canal, represented in red in the above Figure, for the fluid flux that is going to be engraved.

To cut the model and the holes, an acrylic laser cutting machine was used on a 10mm thick crystal clear acrylic plate. This could also be done using a drill bit and a saw, but the laser was chosen for its precision.

For the etching of the canals, that have a depth of approximately 0.5mm, the better option is to also use a laser to engrave the device. Unfortunately, the machine used did not have the precision to etch the canals without cutting the model in half. The solution was to use metal

rods, with length of 2cm and 2.5cm, and thickness of 0.5mm, as shown in Figure 15. The rods were heated using a heating gun and pressed against the acrylic surface. This procedure was done in several spots, until the canals were fully etched.

Figure 15 - Metal rods used for etching

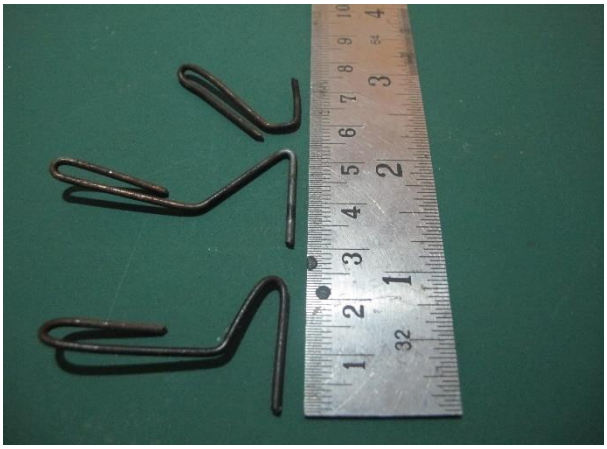

Source: Author (2017).

To make the top tubing connections, a set of bottoming, plug and taper tap were used to thread the acrylic for the tube fittings be able to secure in place.

After the two pieces were cut and etched, they were screwed together using twelve sets of one screw bolt, two washers and one locking nut. On the top of the device, two compression union tube fittings with rubber O-rings were put. The full list of materials is shown in Table 4.

Table 4 - List of materials used for the acrylic device

Part Name	**Part Quantity**	**Part Diameter**
14mm Screw Bolt	8	1/8in DN
18mm Screw Bolt (for corners)	4	1/8in DN
Washer	24	1/8in DN
Locking Nut	12	1/8in DN
Compression Union Tube Fitting	2	1/8in ID and 3/16in OD
Rubber O-Ring	2	3/16in ID
Set of Threading Taps	1	3/16in DN
Plastic Tubing	-	1/8in OD

Source: Author (2017).

A 3D schematic of the pieces used to complete the acrylic model is show in Figures 16 and 17. After the manufacturing and mounting of the device, it is ready to function as a porous medium to study the deposition of mineral scales, as shown in Figure 18.

Figure 16 - 3D Model (Parts)

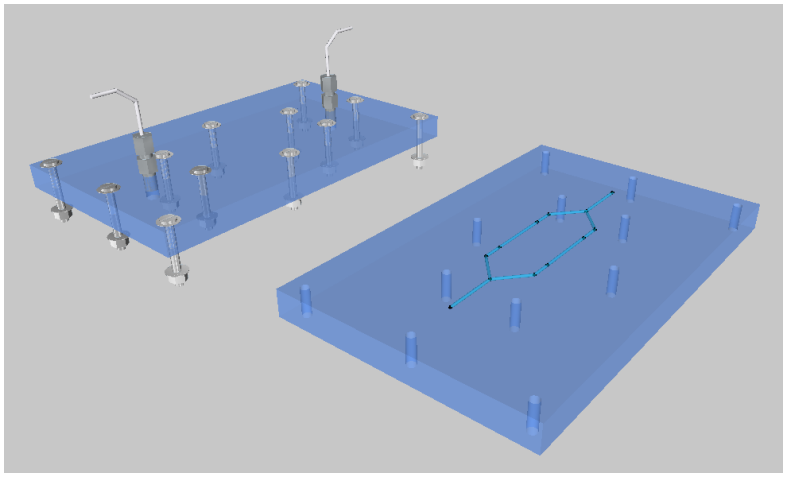

Source: Author (2017).

Figure 17 - 3D Model (Assembled)

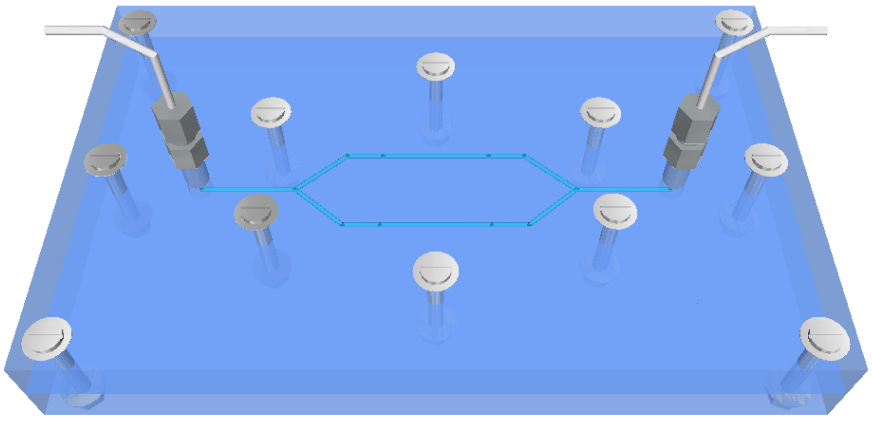

Source: Author (2017).

Figure 18 - Finished acrylic medium

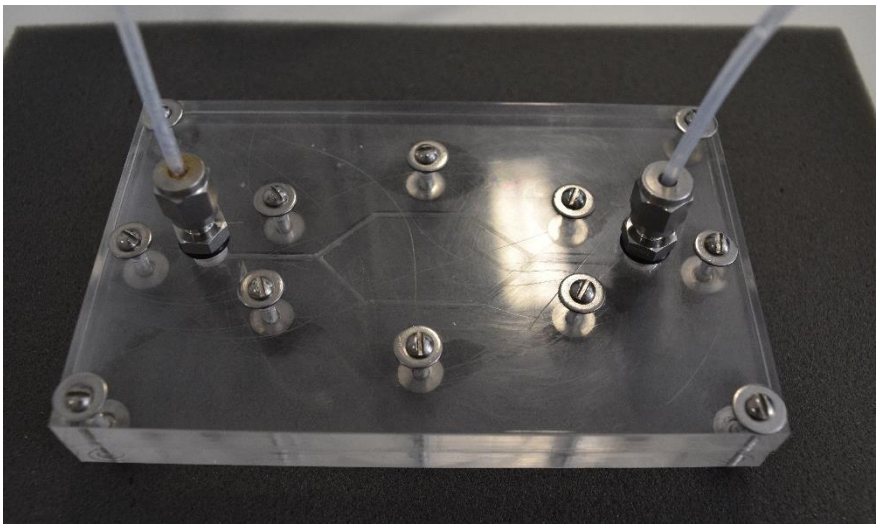

Source: Author (2017).

3.2 Synthetic sea and formation waters

Two liquids were used in this experiment, one being a high salinity composition of formation water, and the other a synthetic injection water. The solutions were made in the laboratory using the salts shown in Figure 19 and Table 5. The salts were weighed inside a 100ml Becker using a Shimadzu AUY220 electronic scale (Figure 20).

Figure 19 - Salts used to prepare the brines

Source: Author (2017).

Table 5 - Salts used to prepare the brines

Salt Name	**Salt Formula**	**Brand**
Sodium Chloride Anhydrous	NaCl	Synth®
Sodium Sulphate Anhydrous	Na_2SO_4	Vetec®
Sodium Bicarbonate Anhydrous	$NaHCO_3$	Vetec®
Calcium Chloride Dihydrate	$CaCl_2.2H_2O$	Vetec®
Magnesium Chloride Hexahydrate	$MgCl_2.6H_2O$	Vetec®
Barium Chloride Dihydrate	$BaCl_2.2H_2O$	Vetec®
Strontium Chloride Hexahydrate	$SrCl_2.6H_2O$	Vetec®
Potassium Chloride	KCl	Vetec®

Source: Author (2017).

The volume of each solution prepared was 500ml, and various mixtures were made with 1000ml each. The changing aspect between each solution was the concentration of the inhibitor that was mixed with the injection water.

The salt contents of each brine (will be shown in the next sections) were weighted and solubilized with 500ml of distilled water in a 1000ml Becker. The formation water solution was added to an 2000ml Becker and then the sea water was added to the same flask, creating the mixture of incompatible waters.

Figure 20 - Shimadzu AUY220 Scale

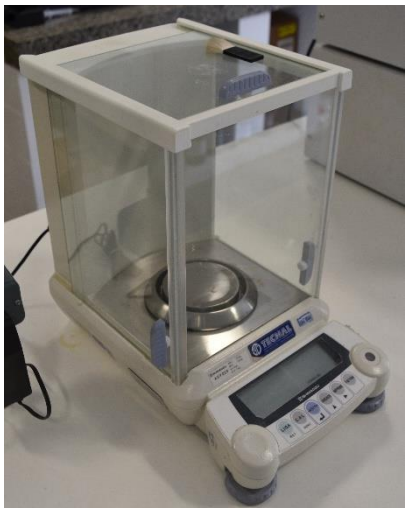

Source: Author (2017).

3.2.1 Formation water composition

Formation water is the brine that resides inside the reservoir rock. In this experiment, two types of formation brines were used. The first one being a high salinity brine (with high concentrations of NaCl, $MgCl_2$ and $CaCl_2$), and the second a high barium concentration brine. These compositions (Table 6) are the same used in Merdhah experiments (MERDHAH, 2007).

Table 6 - Formation water concentration

Salt	**High Salinity Brine**	
	ppm anhydrous	**ppm hydrated**
NaCl	126,073	-
$MgCl_2$	-	37,072
$CaCl_2$	-	27,452
KCl	3,962	-
$SrCl_2$	-	2,684
$BaCl_2$	-	1,804

Source: Merdhah (2007) – Adapted.

The amount weighed of each salt was calculated for a 500ml solution. The mass of each salt is shown in Table 7.

Table 7 - Formation water salt masses

Salt	**High Salinity Brine (g/500ml)**
NaCl	63.03
$MgCl_2$	18.54
$CaCl_2$	13.72
KCl	1.98
$SrCl_2$	1.34
$BaCl_2$	0.90

Source: Author (2017).

3.2.2 Injection water composition

Usually, in offshore or close to the shore onshore wells, the injection water used is commonly just seawater. The average seawater had the composition specified by Millero, when he studied the compositions of various sea brines, as shown in Table 8 (MILLERO, 2006).

However, in this experiment, the injection water used will have a high concentration of NaCl and $NaHCO_3$. The concentration of Na_2SO_4 will be the same as the sea water specified by Millero. The mass and concentrations of the salts used to prepare the injection water is shown in Table 9.

Table 8 - Concentration of ions in sea water

Ion	Concentration (g/kg)
Cl^-	19.3529
Na^+	10.7838
SO_4^{2-}	2.7124
Mg^{2+}	1.2837

Source: Millero (2006).

Table 9 - Mass of salt for injection water

Salt	ppm anhydrous	Mass (g/500ml)
NaCl	123,457	61.72
$NaHCO_3$	3,788	1.89
Na_2SO_4	4,000	2.00

Source: Author (2017).

3.3 Closed-loop system

The experiments were run on a closed-loop system consisting of a pump, the acrylic model and a temperature controlled reservoir. A schematic of the system is shown in Figure 21. The list of the equipment used is:

- Pump: Agilent Technologies Prepstar 218 Solvent Delivery Module
- Pump Head Size: 10WP

- 1/8in OD Plastic Tubing
- 3/16in OD Plastic Fittings
- Acrylic device
- 2000ml Becker (Represented as a Buchner Flask in Figure 21)
- Fisatom 752A Magnetic agitator with heater

Figure 21 - Schematic of the closed-loop system

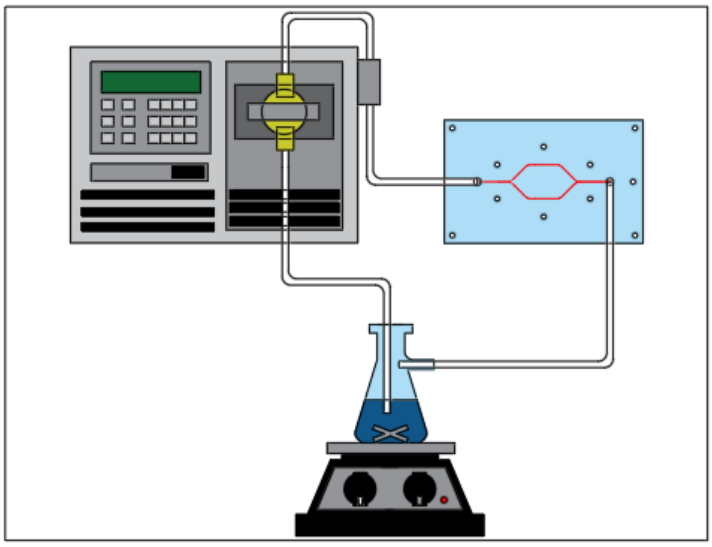

Source: Author (2017).

The tests were all run using a 10ml/min flow rate, with maximum pressure of 30psi. The magnetic agitator was set to a temperature of 50°C and with an agitation level of 4, using a magnetic metal stirrer.

To make sure that the solution in the Becker was not lost due to evaporation, a plastic transparent film was fixed on the top and side holes of the flask. This also prevented dust and other particles from entering the system, making it completely closed. After assembly, the real system is shown below in Figure 22.

Figure 22 - Real system

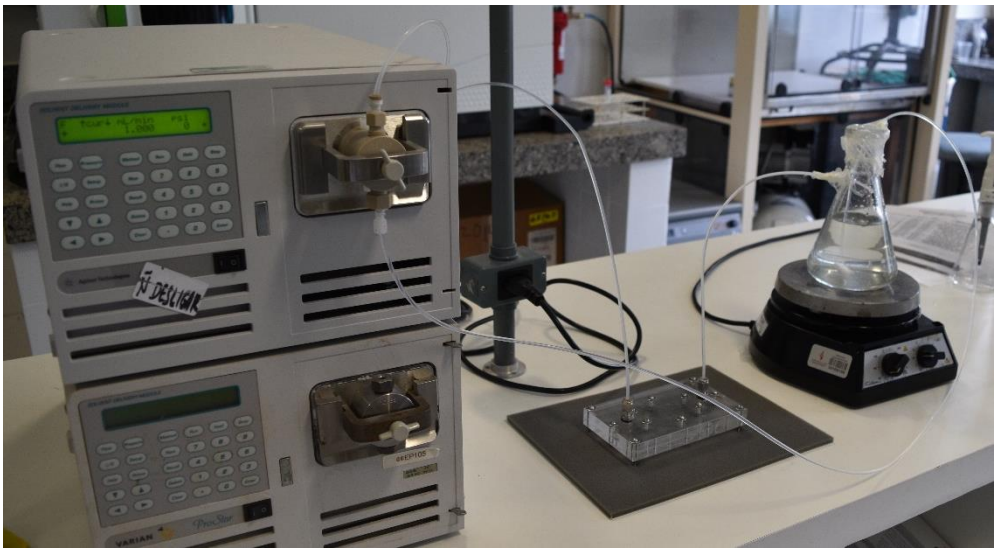

Source: Author (2017).

3.4 ATPM preparation and injection

To prepare the inhibitor solution, first a high concentration solution (128ppm) of ATMP was made with 32mg of ATMP with 250ml of deionized water.

The product used was ATMP (Nitrilotri(methylphosphonic acid)) 97% of the brand Sigma-Aldrich.

This was the chosen method because measuring quantities of low concentrations of ATMP proven to be extremely challenging. The 1, 2, 4, 8, 16ppm solutions were prepared diluting the 128ml solution with the respective quantities of water to achieve the desired concentrations, as shown in Table 10.

Table 10 - ATMP solution preparation

Concentration of ATMP	Volume of 128ppm solution	Volume of water
1 ppm	7.8 ml	992.2 ml
2 ppm	15.6 ml	984.4 ml
4 ppm	31.3 ml	968.7 ml
8 ppm	62.5 ml	937.5 ml
16 ppm	125.0 ml	875.0 ml

Source: Author (2017).

3.5 Sequence of experiments

Following the preparation of the formation water solution, the injection water was prepared using distilled water with the ATMP (tris) inhibitor diluted in it. The concentrations of ATMP and conditions of each test is shown in Table 11.

Table 11 - Experiment Sequence

Concentration of inhibitor	Inhibitor	Temperature	Maximum Pressure
0 ppm	ATMP (tris)	50°C	30 psi
1 ppm	ATMP (tris)	50°C	30 psi
2 ppm	ATMP (tris)	50°C	30 psi
4 ppm	ATMP (tris)	50°C	30 psi
8 ppm	ATMP (tris)	50°C	30 psi
16 ppm	ATMP (tris)	50°C	30 psi
16 ppm	ATMP (tris)	50°C	50 psi

Source: Author (2017).

The experiments using 30psi as a maximum pressure were ran to create a Graph showing the correlation between the concentration of ATMP and the time it took for the liquid inside the acrylic device reach a pressure of 30psi.

The experiment using 16ppm and 50psi as a maximum pressure was ran to show the Pressure x Time correlation when mineral precipitation is blocking the tubes inside the acrylic device.

4 RESULTS AND DISCUSSION

After assembling the handcrafted acrylic chip, two types of experiments were run, the first one to show the correlation between the concentration of methylene phosphonic acid and the time needed for the pressure inside the chip to reach 30psig. This experiment was made using the concentrations of 0, 1, 2, 4, 8 and 16ppm of ATMP inhibitor, at a temperature of 50°C with the injection solution under constant agitation.

The second experiment was to show the correlation between the injection time and the pressure rise inside the acrylic chip. This experiment was made using a concentration of 16ppm of ATMP inhibitor, at a temperature of 50°C with the injection solution under constant agitation. The pump was set to stop when the pressure reached 50psig. The pressure measurements were taken every 10minutes or when a pressure change occurred.

The results for the firsts experiments is shown in Graph 1 and the results for the second experiment is shown in Graph 2. For the second experiment is important to note that the pump only displays discrete values for the pressure, that is why the pressure appears to rise in increments of 10psi.

Graph 1 - Time interval to reach 30psig using different ATMP inhibitor concentrations

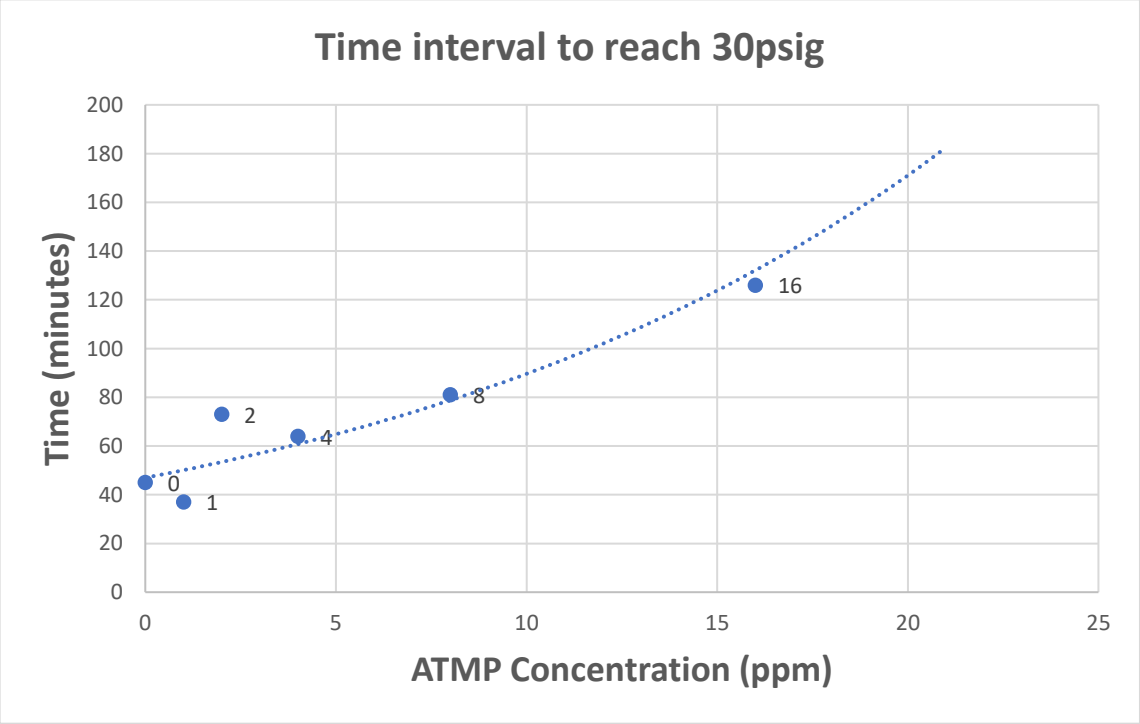

Source: Author (2017).

Graph 2 - Relation between pressure and injection time for 16ppm of ATMP inhibitor

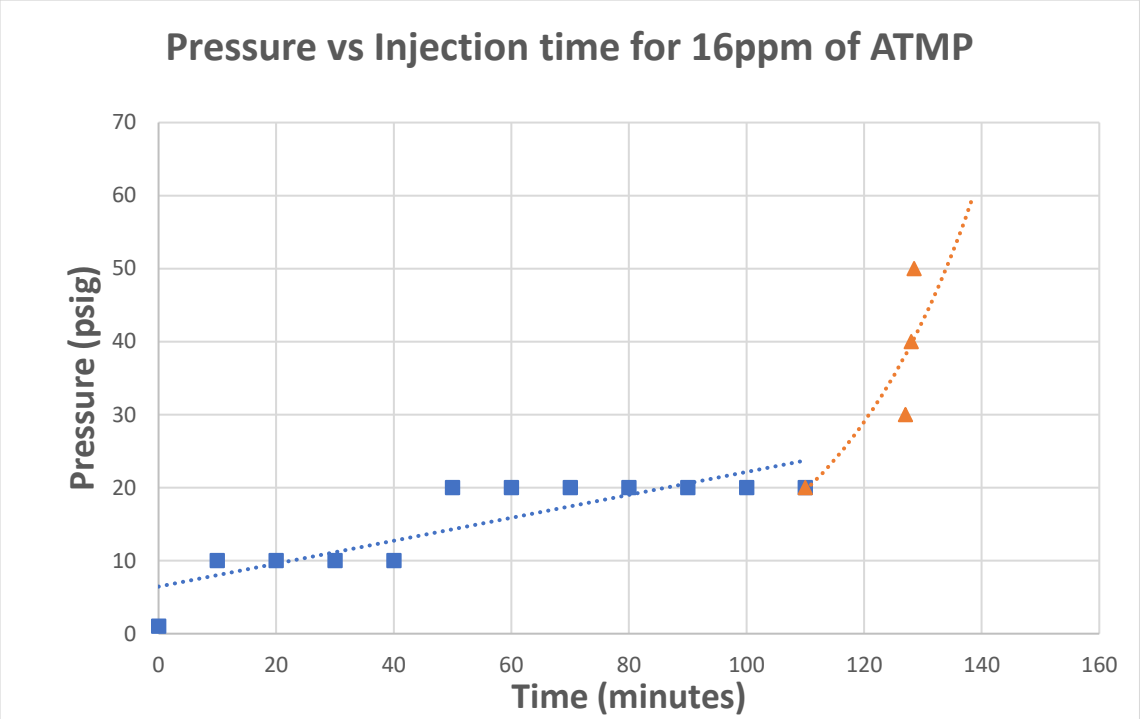

Source: Author (2017).

For the first experiment, we can see that we have a good exponential relationship for the points 0, 4, 8 and 16ppm. Unfortunately, the results for 1 and 2ppm does not follow any logical trend, as it's expected that an increase in inhibitor concentration would make it longer to reach the pressure of 30psig.

The explanation for this should be the precision of the measure instruments, as a concentration of 1 and 2ppm is very small and hard to achieve with good precision. Another cause should be that a concentration of inhibitor below a certain threshold does not make a noticeable difference in time. We can see that above 2ppm, the concentrations start to form a logical and easy to predict trend.

For the second experiment, we can see that we have a logical relationship during all the moments. As it is expected that the pressure rises with the increase of mineral scales inside the acrylic chip.

We can see that we have a somewhat linear trend until the pressure reaches 30psig, from this point the trend is clearly exponential. This happens due to the fact that as the mineral deposits reduces the diameter of the canal, it becomes faster to block the canal, as the area for the mineral to deposit reduces.

During the course of the experiments, several photoGraphs were taken to show the nature and magnitude of the mineral deposition inside the canals of the acrylic porous chip, using a DSLR camera and a microscope.

Figure 23 shows the mineral deposition that can be seen with the naked eye. It was taken using a DSLR camera without zoom, after the injection of the solution with 16ppm of ATMP. We can see at the bottom right corner the spot where a major blockage occurred, stopping the flow from the bottom canal completely.

Figure 24 is a microscope photoGraphy of the canals inside the acrylic chip during two moments, the left image shows a clear canal without deposition and the right image shows the same canal after the experiment with 0ppm of ATMP. The deposition appears in black instead of white because transmitted light was used for those images, so the mineral scales are blocking the light.

Figure 23 – PhotoGraphy of the mineral scales inside the acrylic chip

Source: Author (2017).

Figure 25 is a microscope photoGraphy of the acrylic chip that shows the individual salt crystals that were precipitated and deposited inside the canals. Those crystals start because of a nucleation mechanism and grow as the time passes. In the image we can identify crystals of different sizes, but the majority of them have an average size of 2.5µm to 3.5µm.

Figure 24 - Microscope photoGraphy of the acrylic chip clean (left) and with mineral scales (right)

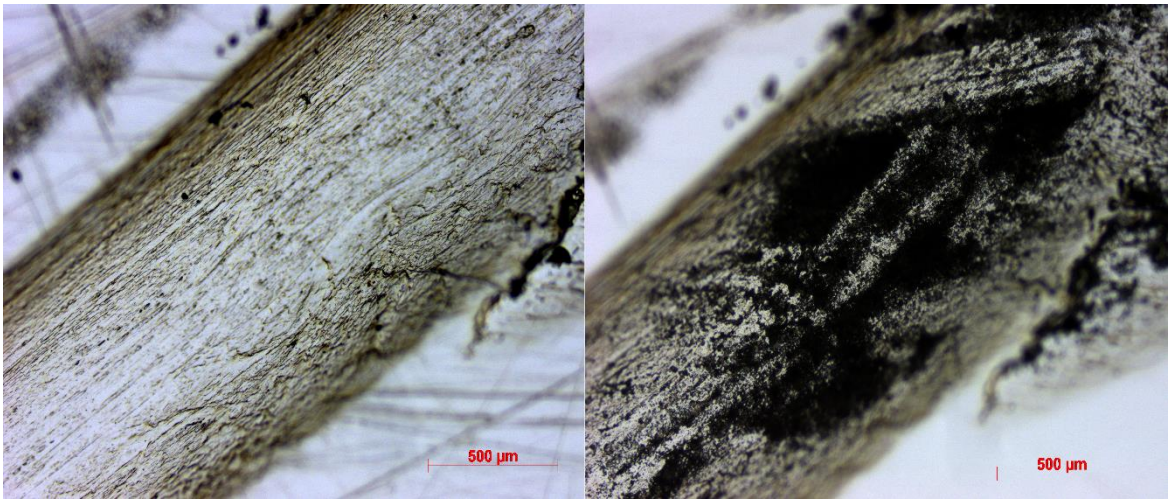

Source: Author (2017).

Figure 25 - Microscope photoGraphy of the precipitated salt crystals inside the acrylic chip

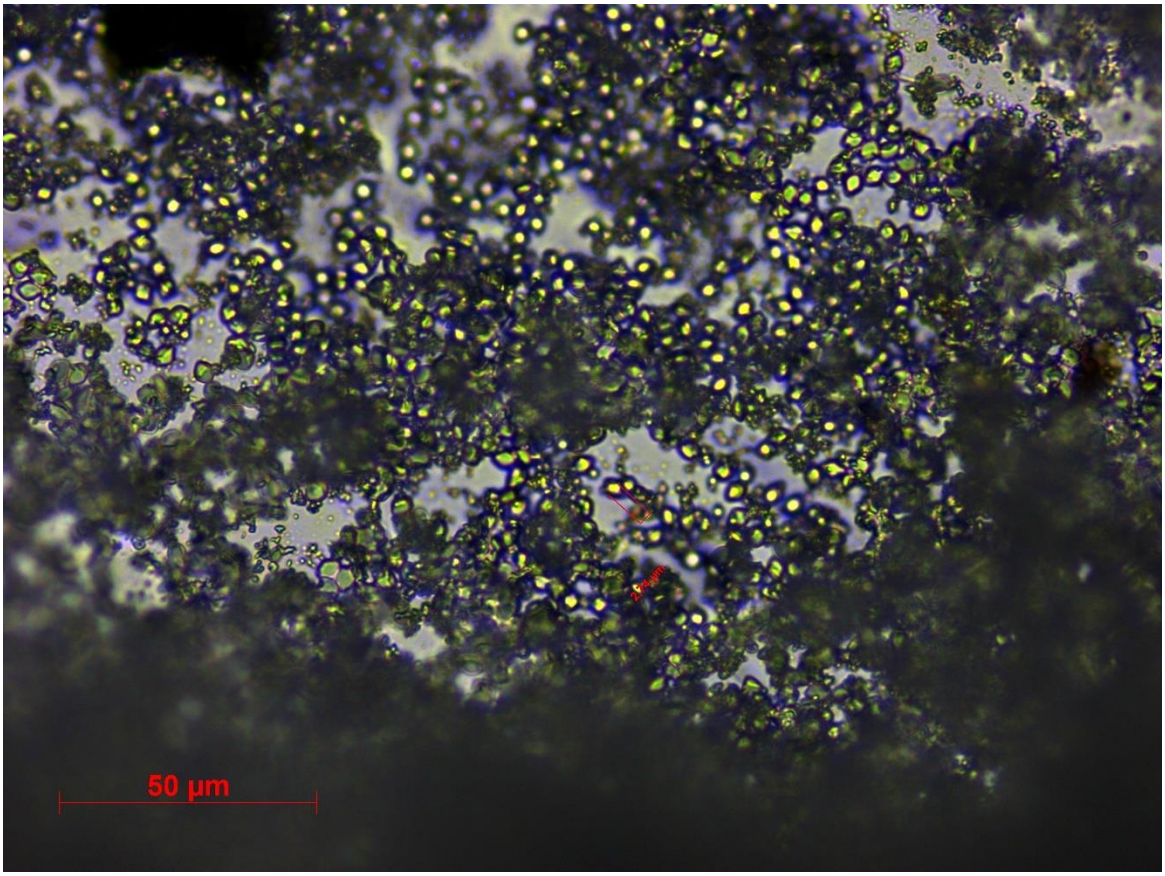

Source: Author (2017).

5 CONCLUSION

It can be concluded from this work that it is possible to design and manufacture an acrylic chip to study the deposition of mineral scales inside tubes. The process of constructing the acrylic chip suffered several modifications since the original idea, but the final iteration of the model was successful in achieving a dispositive to study qualitatively and quantitatively the process of deposition and inhibition of mineral scales.

The quantitative part of this work was experiments that tested the correlation between the time to reach a certain pressure inside the canals and the concentration of inhibitor used, and the experiment to show the correlation of the time of injection and the pressure inside rise inside the canals of the model chip.

Both the quantitative experiments were successful, showing clear trends when analyzing the concentrations of inhibitor and time of brine injection. The first experiment showed an exponential trend of concentration versus time to reach 30psig, and the second experiment showed a linear pressure rise and then an exponential pressure rise when the canal was getting closer to total obstruction.

It is also important to note that the methylene-phosphonic acid was successful in achieving the inhibition of mineral scales, showing a proportional behavior when increasing the concentration versus the time for salt deposition.

The qualitative part of this work was to show that it's possible to visually analyze the deposition of mineral salts using the handcrafted acrylic porous chip. The images presented in the results section clearly shows the formation of crystals and deposition of mineral scales using a camera and a microscope to take pictures.

For future works, it is recommended that more complex designs of the canals are tested, using laser etching or CNC router techniques, to make the canals with machine precision. Also, experiments using different types of inhibitors, temperatures, and solutions for injection and formation water should be ran to have a full knowledge of the subject.

REFERENCES

ATMP. **Wikipedia - The Free Encyclopedia**. Available at: <https://en.wikipedia.org/wiki/ATMP>. Accessed in: 17 December 2017.

BARIUM Sulfate Scale. **FQE Chemicals**. Available at: <https://fqechemicals.com/contaminants/barium-sulfate-scale/>. Accessed in: 17 December 2017.

BARTOLOMEU, L. S. P. **Modelo de Rede de Capilares do Escoamento de Soluções Poliméricas em Meios Porosos**. Pontifícia Universidade Católica. Rio de Janeiro, p. 96. 2017.

BLUNT, M. J.; KING, M. Simulation and theory of two-phase flow in porous media. **A Physical Review**, v. 46, n. 12, 1992.

COSMO, R. D. P. **Modelagem e Simulação Termodinâmica da Precipitação de Calcita em Condições de Poço**. Universidade Federal do Espírito Santo. São Mateus, p. 220. 2013.

CROWE, C. et al. Scale Inhibition in Wellbores. **Society of Petroleum Engineers**, v. doi:10.2118/27996-MS, January 1994.

DOLOMITE. **Data Sheet for Porous Media Chip**. Dolomite Microfluidics. [S.l.], p. 7. 2017.

FATT, I. The network model of porous media. **Petroleum Transactions**, v. 207, p. 144-181, 1956.

GAS Reservoir. **Encyclopaedia Britannica**, 2010. Available at: <https://www.britannica.com/science/gas-reservoir>. Accessed in: 17 December 2017.

KELLAND, M. A. Effect of Various Cations on the Formation of Calcium Carbonate and Barium Sulfate Scale with and without Scale Inhibitors. **Industrial & Engineering Chemistry Research**, v. 50, n. 9, p. 5852-5861, 2011.

MERDHAH, A. B. M. B. **The Study of Scale Formation in Oil Reservoir During Water Injection at High-Barium and High-Salinity Formation Water**. Universiti Teknologi Malaysia. [S.l.], p. 189. 2007.

MILLERO, F. J. **Chemical OceanoGraphy**. [S.l.]. 2006.

ODDO, J. E.; SMITH, J. P.; TOMSON, M. B. Analysis of and Solutions to the CaCO3 and CaSO4 Scaling Problems Encountered in Wells Offshore Indonesia. **Society of Petroleum Engineers**, v. doi:10.2118/22782-MS, January 1991.

OLIVEIRA, A. R. C. D. **Avaliação de Métodos de Seleção de Anti-Incrustantes Fosfonatados Para Reservatórios de Petróleo**. Universidade Federal do Ceará. Fortaleza, p. 84. 2017.

SCALE Control. **Aquatek Pro**. Available at: <http://www.aquatekpro.com/index.php/quality-water-benefits/scale-control>. Accessed in: 17 December 2017.

TOMSON, M. B. et al. Mechanisms Of Mineral Scale Inhibition. **Tomson, M. B.; Fu, G.; Watson, M. A.; Kan, A. T.**, v. doi:10.2118/74656-MS, January 2002.

TOMSON, M. B. et al. A Molecular Theory Of Mineral Scale Inhibition. **NACE International**, January 2004.

VELOSO, C. B. **Avaliação dos Mecanismos de Adsorção e Precipitação de Inibidores de Incrustação em Rocha Arenítica Por Meio de Ensaios Estáticos e Dinâmicos**. Universidade Federal do Ceará. Fortaleza, p. 128. 2017.